

Rod Cells Dissociated from Mature Salamander Retina: Ultrastructure and Uptake of Horseradish Peroxidase

E. TOWNES-ANDERSON, P. R. MACLEISH,* and E. RAVIOLA

Departments of Anatomy and *Neurobiology, Harvard Medical School, Boston, Massachusetts 02115.

Dr. MacLeish's present address is The Rockefeller University, New York 10021.

ABSTRACT To test the effects of isolation on adult neurons, we investigated the fine structure and synaptic activity of rod cells dissociated from the mature salamander retina and maintained *in vitro*. First, freshly isolated rod cells appeared remarkably similar to their counterparts in the intact retina: the outer segment retained its stack of membranous disks and the inner segment contained its normal complements of organelles. Some reorganization of the cell surface, however, was observed: (a) radial fins, present at the level of the cell body, were lost; and (b) the apical and distal surfaces of the inner and outer segments, respectively became broadly fused. Second, the synaptic endings or pedicles retained their presynaptic active zones: reconstruction of serially sectioned pedicles by using three-dimensional computer graphics revealed that 73% of the synaptic ribbons remained attached to the plasmalemma either at the cell surface or along its invaginations. Finally, tracer experiments that used horseradish peroxidase demonstrated that dissociated rod cells recycled synaptic vesicle membrane in the dark and thus probably released transmitter by exocytosis. Under optimal conditions, a maximum of 40% of the synaptic vesicles within the pedicle were labeled. As in the intact retina, uptake of horseradish peroxidase was suppressed by light. Thus, freshly dissociated receptor neurons retained many of their adult morphological and physiological characteristics. In long-term culture, the photoreceptors tended to round up; however, active zones were present even 2 wk after removal of the postsynaptic processes.

Rod cells from the tiger salamander are ideally suited for the study of the cell biology of isolated adult neurons: they survive intact after dissociation (1); they can be maintained in culture for long periods of time (2); and they give normal hyperpolarizing responses to light (1). Although the electrical responses of these cells have been studied in some detail (3–5), a number of crucial properties are still unknown; it seems especially important to establish whether solitary rod cells, maintained *in vitro*, preserve their morphologically differentiated state and whether their synaptic endings retain functional active zones capable of releasing transmitter by exocytosis in the dark.

In this paper, the fine structure of salamander rod cells was compared in the intact retina and after dissociation. The geometry of the active zones in the synaptic terminals of solitary rod cells was analyzed by three-dimensional computer graphic reconstruction of serial sections. Finally, the functional state of their endings was tested by observing the uptake of the extracellular tracer, horseradish peroxidase, into synaptic vesicles. Portions of this work have appeared in preliminary form (2, 6, 7).

MATERIALS AND METHODS

Animals: Aquatic-phase salamanders (*Ambystoma tigrinum*) measuring from 18 to 25 cm in total length were used. Animals of this size, although in the aquatic or larval phase, are considered adult inasmuch as *Ambystomidae* are both neotenic and paedogenic (8). The salamanders were maintained at 5°C on a 12-h light/12-h dark cycle. They were sacrificed after either 5 h of light exposure or 2 or more hours of dark adaptation.

Electron Microscopy of Intact Retina: Light-adapted animals were decapitated and pithed. Primary fixative was applied to the outer surface of the eye and surrounding tissue. After 5 min, the eyes were enucleated, left in fixative for an additional 15 min, and then transected at the equator. Eyecups were fixed for 1 h at room temperature. Primary fixative was 2.5–4% glutaraldehyde, 2.5% paraformaldehyde in 0.07 M Sörensen's phosphate, or 0.1 M cacodylate buffer at pH 7.4; for one specimen, 0.05% picric acid was added to the primary fixative. The eyecups were rinsed, the scleras were removed, and the retinas were cut into small pieces and postfixed in a solution of 1% OsO₄, 1.5% potassium ferrocyanide (9) for 1 h at room temperature. Tissue was stained en bloc with 1% uranyl acetate in maleate buffer, dehydrated, and embedded in an Epon-Araldite mixture. Thin sections were placed on Gilder grids (Marivac Services, Halifax, Nova Scotia), stained with uranyl acetate and lead citrate, and viewed in a JEOL-100B electron microscope (JEOL USA, Electron Optics Div., Peabody, MA).

Cell Dissociation and Maintenance: The procedures followed those described by Lam (10) and Bader et al. (1) with some modifications. Cell

isolation was done either under normal fluorescent room light or very dim red light. Light- or dark-adapted salamanders were decapitated and pithed. Eyes were enucleated and transected, and the retinas were gently removed and placed in an enzyme solution that contained 85 mM NaCl, 25 mM NaHCO₃, 1.5 mM KCl, 1.8 mM CaCl₂, 0.5 mM NaH₂PO₄, 16 mM glucose, 1.0 mM Na pyruvate, 2.7 mM cysteine, and 14 U/ml papain (catalogue no. 3126, Worthington Biochemical Corp., Freehold, NJ); the solution was bubbled with 5% CO₂, 95% O₂ shortly before use. Retinas were incubated at 30°C for 30 min with gentle agitation and then rinsed three times. The salt solution used for rinsing contained 108 mM NaCl, 2.5 mM KCl, 1.0 mM NaHCO₃, 0.5 mM NaH₂PO₄, 16 mM glucose, 1.0 mM Na pyruvate, 0.5 mM MgSO₄, and from 0.225 to 1.8 mM CaCl₂; it was buffered with 2 mM HEPES adjusted to pH 7.7 with NaOH and gassed with 100% O₂. Retinas were gently triturated in 1 ml of the salt solution, and a population of cells containing rod and cone photoreceptors and Müller cells was obtained. Aliquots of the cell suspension were placed into either round-bottomed test tubes or shallow wells made from petri dishes that were fitted with polystyrene or Thermanox (Miles Laboratories, Naperville, IL) coverslips (11). Cells were maintained in 1–2 ml of salt solution on a Peltier device. For short-term culture (up to 2 h), temperature was kept at 10, 18, or 22°C; 0.1 mg/ml BSA or NuSerum (Collaborative Research, Inc., Lexington, MA) was added to the salt solution in some cases. For long-term culture (up to 2 wk), the salt solution was supplemented with 0.1 mM choline and 0.1 mg/ml gentamicin, and the cells maintained at 10°C in a humid, oxygenated atmosphere; cultures were kept in the dark except when their medium was changed or they were examined with the light microscope.

Electron Microscopy of Dissociated Cells: Cells were fixed 1 and 2 h after dissociation or after 24 h, 1 wk, and 2 wk of culture. For primary fixation, an equal volume of 2.5% glutaraldehyde, 2.5% paraformaldehyde, and 0.05% trinitroresol or picric acid (12) in 0.07 M Sørensen's phosphate or 0.1 M cacodylate buffer, pH 7.4, was added to the culture medium, and the cells were allowed to come to room temperature. After 1 h, fixative fluid was carefully removed and the cells, which remained in a single layer on the bottom of the well, were embedded in a very thin layer of 1% agarose (type VII, Sigma Chemical Co., St. Louis, MO). For cells that had been fixed in test tubes, it was necessary to transfer the cells to modified petri dishes and allow them to settle on the bottom surface of the well before embedding in agarose. Cells were postfixed and stained en bloc as above. The thin agarose disks that contained the cells were removed from the petri dishes during dehydration and embedded in an Epon-Araldite mixture. The insoluble Thermanox coverslips were removed from the agarose disks after polymerization of the plastic. Individual cells or groups of cells were selected for thin sectioning by viewing plastic embedded disks in the light microscope. With this procedure it was possible (a) to identify intact photoreceptors and (b) to obtain longitudinal sections of entire receptor cells.

Serial Reconstruction of Synaptic Terminals: For two rod cells, dissociated from light-adapted retinas and maintained in the light for 2 h at 10°C, the synaptic ending or pedicle was serially sectioned, placed on Formvar-coated slotted grids, stained with uranyl acetate and lead citrate, and examined in the electron microscope. Micrographs were taken of each section and printed at a final magnification of 20,000. From the prints, tracings were made of the following structures: (a) the plasmalemma of the ending; (b) all large and small membranous profiles within the ending that were associated with synaptic ribbons; (c) large membranous profiles with no associated ribbons; and (d) all synaptic ribbons. Successive tracings were placed in register with one another and their mutual orientations were marked with three dots. Pedicles were subsequently reconstructed from the tracings by three-dimensional computer graphics (the computer graphics system was constructed in the Neurobiology Department of Harvard Medical School; for a brief description see reference 13).

Horseradish Peroxidase Uptake: Isolated rod photoreceptors were incubated in the salt solution containing 0.7% horseradish peroxidase (HRP¹;

¹ Abbreviation used in this paper: HRP, horseradish peroxidase.

type II, Sigma Chemical Co., or grade I, Boehringer Mannheim Biochemicals, Indianapolis, IN) for 30 min in the dark or under continuous illumination. White light (color temperature 3,400°K) was delivered from an 80-W tungsten quartz-iodine lamp by an 11-80 Fiber Optic Illuminator (American Optical Corp., Southbridge, MA). Irradiance, measured by a calibrated silicon photodiode, was 7.22 W/m².

Cells were subsequently fixed as specified above either in the dark or the light, embedded in agarose, and processed for the histochemical demonstration of HRP according to the method of Graham and Karnovsky (14) or by a more recent modification that uses cobalt chloride intensification (15). Reacted agarose disks were prepared for electron microscopy as described above.

RESULTS

Rod Cells in the Intact Retina

Rod cells make up approximately half of the photoreceptor layer in the salamander retina (16). Both red and green rod photoreceptors are present although green rods are estimated to be <10% of the total rod cell population (5). Because of the scarcity of green rod cells, the following description refers to red rod photoreceptors.

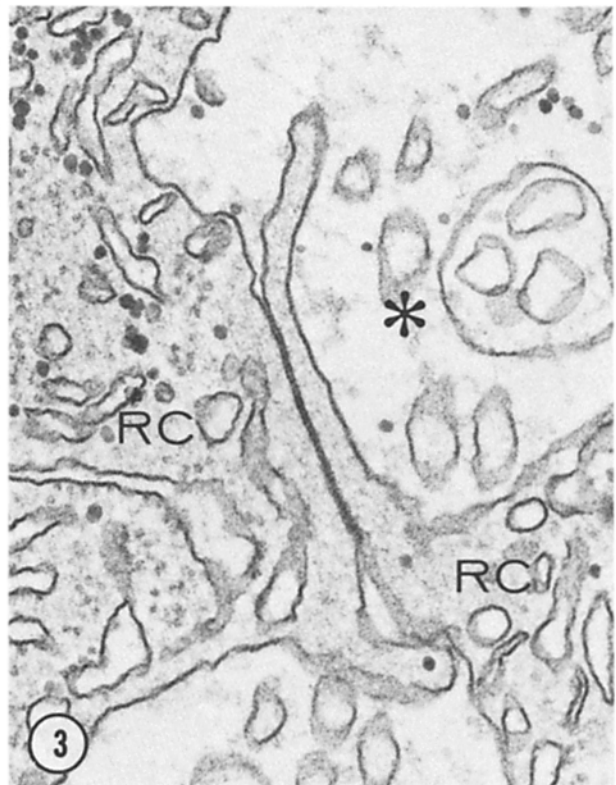
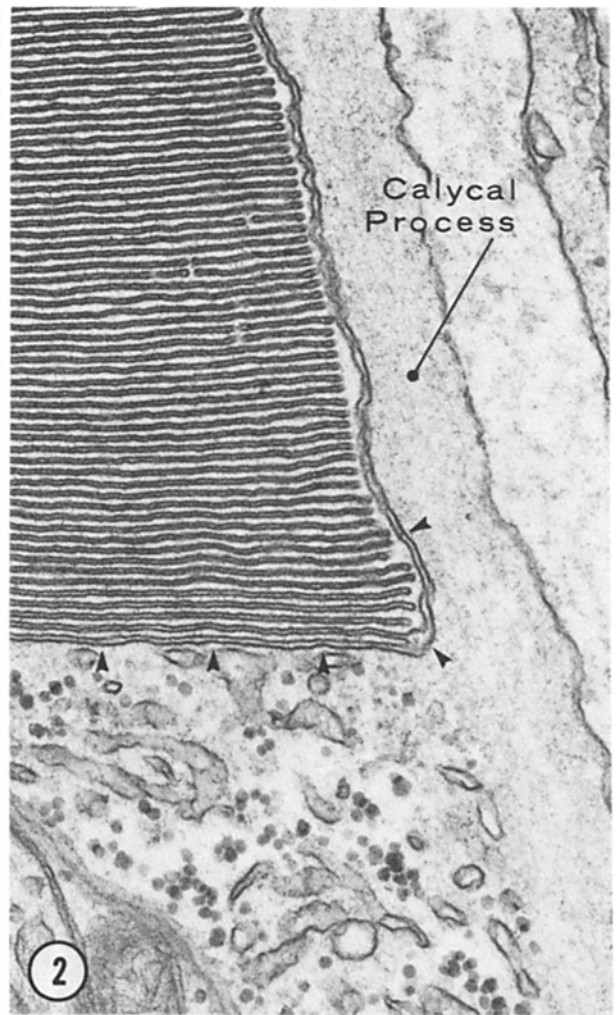
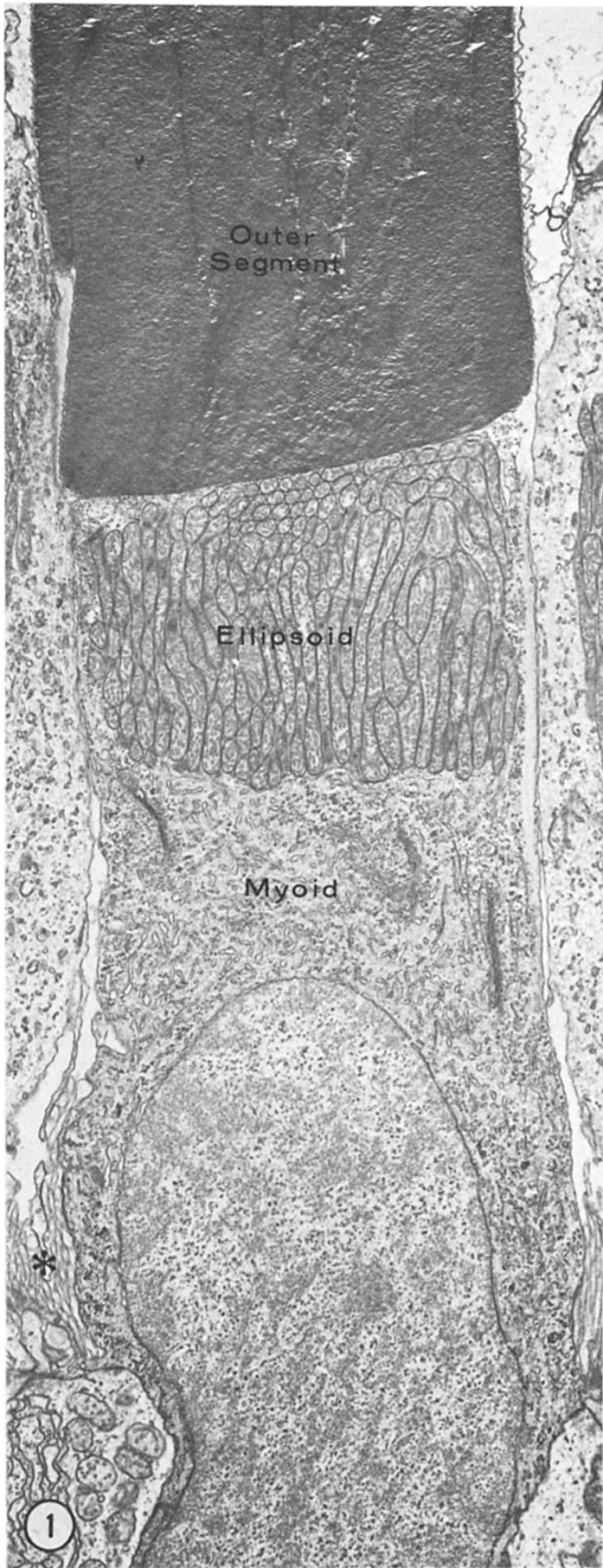
In the red rod cell, the outer segment constituted approximately one-third of the total length of the photoreceptor and was cylindrical in shape. The inner segment, although shorter in length, had the same diameter as the outer segment; it was subdivided into a large ellipsoid, at the base of the outer segment, and a short myoid region between the ellipsoid and the cell body. The perikaryon, containing an angular nucleus, was located at the level of the outer limiting membrane and gave rise to a thin fiber that terminated with a synaptic ending or pedicle in the outer plexiform layer.

The outer segment of the rod cell (Figs. 1 and 2) consisted of a stack of membranous disks enclosed within the plasmalemma. Each disk had a scalloped contour and was segmented into lobes by shallow incisures. The lobulations of the disks were in register with one another creating grooves along the surface of the outer segment; in the basal fourth of the outer segment, calyceal processes, originating from the inner segment, occupied these grooves.

The inner segment (Fig. 1) was characterized by an abundance of cytoplasmic organelles and inclusions: the ellipsoid was made up of a very tightly packed accumulation of mitochondria and was circumscribed by a loose network of smooth endoplasmic reticulum; the myoid contained a prominent Golgi apparatus, rough and smooth endoplasmic reticulum, free ribosomes, glycogen particles, lysosomes, and cytoskeletal elements. The calyceal processes were filled with fine filaments; these filaments extended for several micrometers into the inner segment, lying just underneath the cell membrane (Fig. 2).

As in most vertebrates, inner and outer segments were connected by an asymmetrically located cilium. Thus, most of the base of the outer segment was separated from the apical

FIGURES 1–3 Intact retina. Fig. 1: The scleral portion of the rod cell is made up by an outer and inner segment. The outer segment contains a stack of membranous disks. The inner segment consists of the ellipsoid, characterized by an accumulation of mitochondria, and the myoid, a region rich in cell organelles, which contains a prominent Golgi apparatus. The myoid is in turn continuous with the cell body where the nucleus is located. Above the external limiting membrane, the photoreceptor cells project lamellar processes or fins that interdigitate with the apical microvilli of Müller cells (*asterisk*, this region is enlarged in Fig. 3). $\times 5,600$. Fig. 2: The inner and outer segments are separated by a narrow cleft, which is continuous with the extracellular space and the cleft intervening between the calyceal process and the outer segment (*arrowheads*). In the outer segment, the membranous disks are enclosed by the plasmalemma; the calyceal process is filled with a filamentous mat that extends down into the inner segment. $\times 45,800$. Fig. 3: The fins of adjacent photoreceptors are joined by gap junctions. The extracellular space (*asterisk*) between rod cells (RC) contains Müller cell processes, here cut in cross section. $\times 74,000$.



surface of the inner segment by a narrow cleft that was continuous with the interreceptor space (Fig. 2). A similar, narrow, extracellular cleft separated the lateral surface of the outer segment from the calyceal processes.

At the cell body, the surface of the photoreceptor expanded into a series of lateral projections or fins. These fins were generally devoid of cell organelles although small membrane-bound vesicles or vacuoles were occasionally present. Fins from adjacent photoreceptors interdigitated in a gearlike fashion; as in *Ambystoma mexicanum* (17), numerous gap junctions were present both between the fins of adjacent rod cells (Fig. 3) and between adjacent rod and cone cells.

The synaptic endings of tiger salamander rod cells possessed one or more pedicles. Multiple pedicles were joined to the cell body either by a common fiber or by separate fibers; two pedicles could also follow each other in sequence along the length of the same fiber (18). The fiber that extended into the outer plexiform layer had abundant microtubules, elements of the endoplasmic reticulum, glycogen granules, and a few small vesicles. In the pedicles (Fig. 4), synaptic vesicles, measuring 40–50 nm in diameter, were the dominant cell organelle although profiles of agranular reticulum, glycogen, and microtubules were also present. Both thick, basal processes and thin, fingerlike filopodia extended from the pedicles. The basal processes (Fig. 5), like the fiber, had more microtubules and fewer vesicles than the pedicle, whereas the filopodia were filled by a fine filamentous matrix and scattered vesicles. At their base, the pedicles made synaptic junctions with second order neurons and cone cells; some synapses were also observed between basal processes and unidentified elements (Fig. 5). In the tiger salamander, these junctions have been divided into three groups (18): distal junctions, basal junctions, and ribbon synapses. Distal and basal junctions were marked by a paucity of synaptic vesicles near the pedicle membrane, a wide synaptic cleft containing opaque material and, limited to the basal junctions, a dense undercoating of the pedicle membrane (Fig. 6). At the ribbon synapse, the postsynaptic processes usually occupied an invagination of the rod synaptic ending (Fig. 4); the pedicle sent a wedge-shaped projection or synaptic ridge between them. The synaptic ridge was bisected by the ribbon which in turn was surrounded by a halo of synaptic vesicles (Fig. 7). A small, diffuse, arciform density was present between the ribbon and the plasmalemma at the apex of the ridge.

Freshly Dissociated Rod Cells

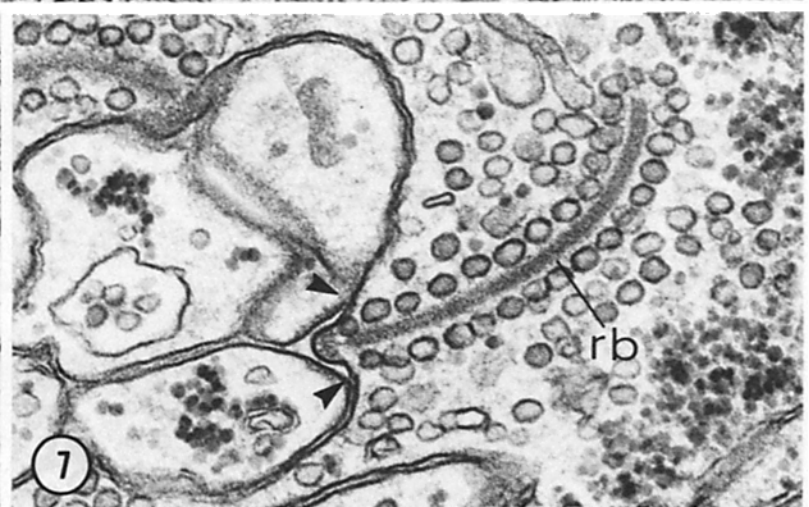
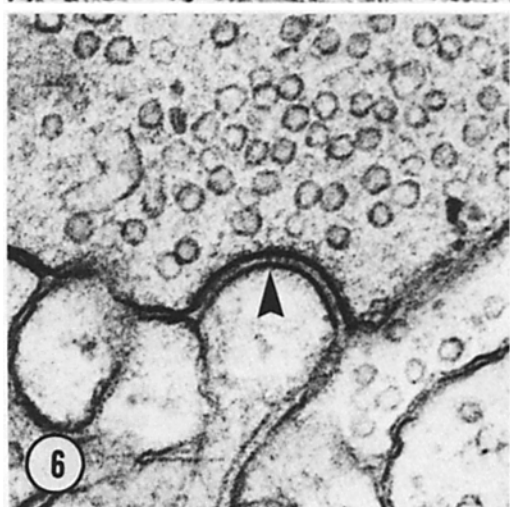
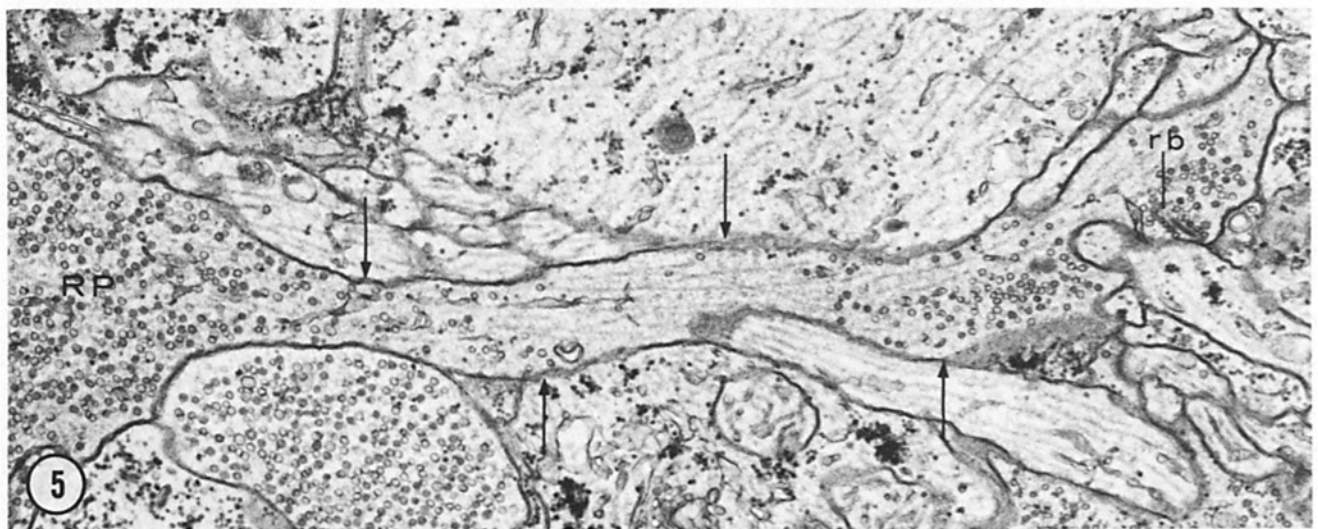
1–2 h after dissociation, the majority of the isolated rod cells appeared intact when examined with the light microscope. A variable proportion of them, however, had lost either their outer segment or their pedicle. With the electron microscope, intact rod cells looked remarkably similar to their counterparts in the intact retina. Most nuclei, however, were

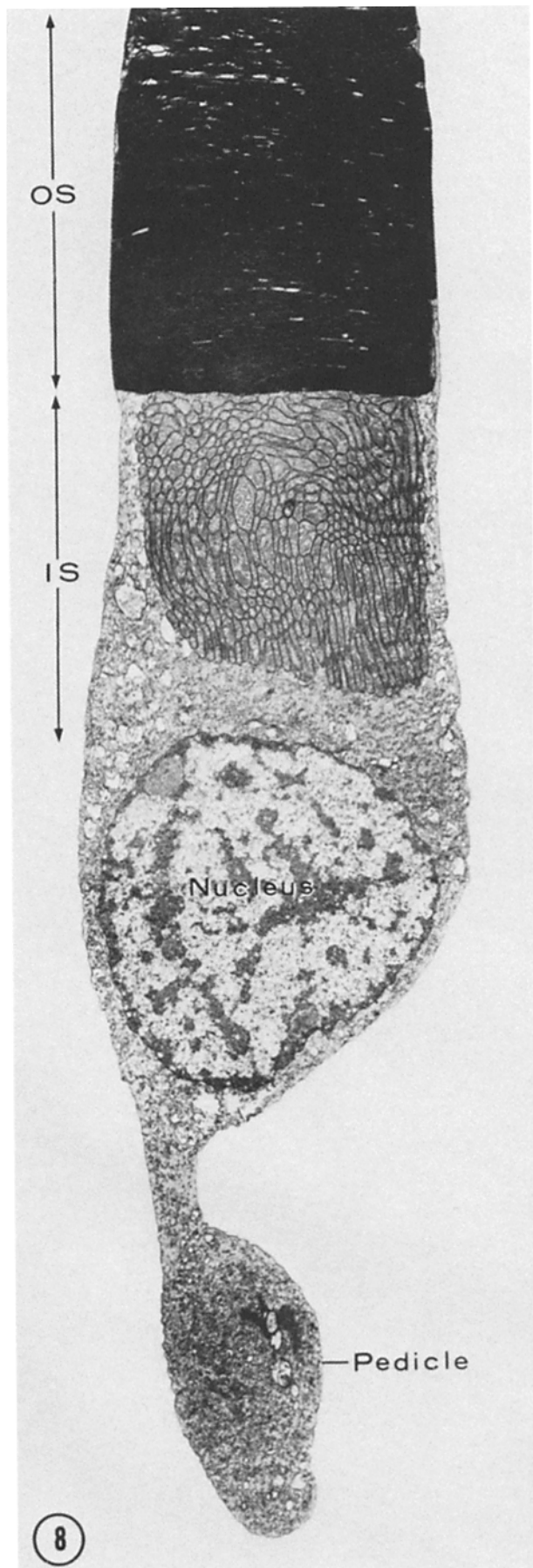
now oval in shape and the synaptic endings appeared to have rounded up (Fig. 8). The outer segment maintained its stack of tightly packed membranous disks and the inner segment contained its normal complement of cytoplasmic organelles and inclusions (Figs. 9 and 10). Some alterations of the rod cell surface, however, occurred. First, the narrow extracellular cleft that separated the outer from the inner segment in the intact retina had disappeared (Fig. 11). Instead, the apical surface of the inner segment and the basal surface of the outer segment appeared to have fused so that the lowermost disk of the outer segment was in direct contact with the cytoplasm of the inner segment. In dissociated cells incubated with HRP, tracer was never found between the inner and outer segments; this is in contrast to the intact retina where HRP has been shown to fill the cleft between these two regions of the photoreceptor (19). This process of membrane fusion included the calyceal processes: their fine filamentous matrix was still visible but their outer membrane had become continuous with the plasmalemma of the outer segment. Moreover, at the boundary region between the inner and outer segment, and between the remnants of the calyceal processes and the membranous disks, a row of flattened membranous sacs was often seen. These sacs could represent vestiges of the apposed membrane of the inner and outer segments. A second alteration occurred at the level of the cell body: laterally projecting fins were no longer present. Instead, in some rod cells, there was a transient accumulation of phagocytic vacuoles in the myoid region and cell body immediately after the dissociation procedure (Fig. 8); 2 h after dissociation, most vacuoles had disappeared (Fig. 9).

The fine structure of the rod cell fiber remained unchanged after dissociation (Fig. 12). Some rod cells, however, lacked a fiber. It is possible that during dissociation, the fiber retracted or merged with the cell body and the pedicle came to lie like a crescent of cytoplasm over the basal surface of the nucleus. Some of these cells, however, may have been rod photoreceptors, which in the intact retina did not possess a fiber. Likely candidates were the green rod cells and a few red rod cells whose nuclei were situated within the layer of cone cell nuclei and thus close to the outer plexiform layer.

The surface of the synaptic terminals of freshly dissociated rod cells was consistently free of adhering cellular debris (Figs. 12 and 13); in addition, the cleft material found at distal and basal junctions had disappeared. The dense undercoating that was associated with the pedicle membrane at basal junctions could not be identified; this may be due either to the diffuse nature of this membrane-associated cytoplasmic dense material or the disappearance of this material after dissociation. The pedicles contained synaptic ribbons, synaptic vesicles, small vacuoles, a few scattered profiles of endoplasmic reticulum, glycogen particles, and cytoskeletal elements (Figs. 12–14). Synaptic ribbons retained their pentalaminar structure

FIGURES 4–7 Intact retina. Fig. 4: The synaptic ending or pedicle of the rod cell is filled with synaptic vesicles and contains synaptic ribbons (*rb*). At the ribbon synapse, postsynaptic processes invaginate the surface of the ending (*arrowheads*). $\times 20,000$. Fig. 5: A basal process (*arrows*) extends from the rod pedicle (*RP*) into the surrounding neuropil. In contrast to the pedicle, the process contains numerous microtubules and few vesicles; small synaptic ribbons are also present (*rb*). $\times 16,100$. Fig. 6: At the basal junction (*arrowhead*), the rod pedicle contacts a single process. The junction is marked by a 12-nm intercellular cleft containing opaque material and a dense undercoating along the cytoplasmic surface of the pedicle membrane. $\times 90,000$. Fig. 7: At the ribbon synapse, the synaptic ridge (located between the *arrowheads*) is wedge-shaped, thus allowing the rod pedicle to contact two postsynaptic processes. The presynaptic active zone is characterized by a synaptic ribbon (*rb*) surrounded by synaptic vesicles and associated with the plasmalemma by a small, arciform density, located at the apex of the synaptic ridge. $\times 78,800$.





and were surrounded by a halo of synaptic vesicles. Many ribbons were associated with the plasmalemma (Fig. 13); as in the intact retina, this association was frequently mediated by a rudimentary arciform density. Very rarely, the plasmalemma formed a small, rounded elevation at the arciform density, but in most cases the synaptic ridge had completely flattened out. In random thin sections, ribbons were also seen in the cytoplasm and appeared connected to large or small, circular, or flattened membranous profiles (Fig. 14).

Serial reconstructions of two synaptic endings were used to determine whether the membranous profiles associated with synaptic ribbons were endocytic vacuoles or cross sections of invaginations of the cell membrane. One ending consisted of a single pedicle (Fig. 15), the other contained two pedicles attached to the cell body by a common fiber (Fig. 16). In both cases, the pedicles were rounded in contour, and gave rise to large and small processes. On the basis of their fine structure, the large processes appeared equivalent to the basal processes found in the intact retina. From the serial thin sections, it was clear that virtually all the synaptic ribbons retained their connection either to the plasmalemma or to cytoplasmic membranous profiles. A few small ribbons were also present in basal processes as observed in the intact retina (Fig. 5). Three-dimensional computer graphic reconstruction of the pedicles, which allows the endings to be viewed at any desired angle, demonstrated that large circular or flattened membranous profiles that appeared isolated in the cytoplasm in random thin sections actually represented elongate sacs that opened out to the extracellular space (Figs. 17 and 18); this suggested that some of the invaginations of the pedicle surface that contained the teleodendria of second-order neurons in the intact retina, were retained after dissociation. For the smaller membranous profiles, no connection with the cell surface could be found; these profiles, therefore, seemed to represent endocytic vacuoles. In each pedicle, the number of synaptic ribbons attached to endocytic vacuoles, and thus removed from the surface of the ending, was small (Table I). In fact, 73% of the ribbons remained attached to the plasmalemma either at the cell surface or along its invaginations.

Serial reconstruction also demonstrated that although ribbons had a constant thickness of 27 nm, they varied in both width and length. This result agreed with our observations on random thin sections of rod pedicles from the intact retina.

At the fine structural level, no significant variations were observed between cells of the same dissociation. Furthermore, the morphology of freshly dissociated cells did not vary substantially with changes in temperature (10–22°C) or medium (see Materials and Methods). Finally, the loss of either the outer segment or the pedicle did not result in noticeable alterations in the structure of the remaining portion of the cell.

Uptake of HRP

Freshly isolated rod cells, incubated with HRP for 30 min in the dark, took up the tracer into their synaptic terminals (Fig. 19). HRP was present within synaptic vesicles, coated

FIGURE 8 Freshly dissociated rod cell. The photoreceptor cell closely resembles its counterpart in the intact retina. The fins, however, are absent and numerous vacuoles occur near the surface of the inner segment (IS). OS, outer segment. $\times 3,800$.

vesicles, and occasionally in small vacuoles. Labeled synaptic vesicles were randomly distributed throughout the cytoplasm of the pedicle and some were associated with synaptic ribbons (Fig. 19, *inset*). Pedicles connected to the cell body by a fiber and those adjacent to the base of the nucleus were equally able to pick up the tracer; in both cases, labeled vesicles were sometimes observed in the cell body but never in the myoid region of the rod cell.

A series of experimental conditions were tried to enhance the uptake of HRP by the endings in the dark: photoreceptors were dissociated from either light- or dark-adapted animals; dissociation was done either in room light or in the dark; incubation with HRP immediately followed dissociation or receptors were left to recover in the culture medium for various time intervals up to 1 h before exposure to the tracer; finally, the CaCl_2 concentration was varied from 0.225 to 1.8 mM and the temperature of the medium was maintained at 10, 18, or 22°C. Some vesicle labeling was observed in all conditions, except when cells were exposed for 1 h or more to temperatures of 18 or 22°C, which completely inhibited tracer uptake. The largest number of pedicles containing HRP-filled vesicles and the highest proportion of labeled vesicles within each pedicle was obtained with the following protocol: (a) cells were dissociated in room light from light-adapted animals; (b) they were cultured for 1 h in the light before incubation with HRP in the dark; (c) culture medium contained a concentration of CaCl_2 of 0.9 mM or less; and (d) temperature was maintained at 10°C. Under these conditions, it was consistently possible to label 40% of the vesicles.

The effects of light were tested on the preparations in which incorporation of HRP was maximal in the dark. Light exposure during incubation with tracer completely suppressed the uptake of HRP by solitary rod cells (Fig. 20). In comparison with the endings incubated in the dark, the synaptic vesicles appeared to congregate in tightly packed aggregates, separated by islands of homogeneous cytoplasmic matrix. In addition, there was an increase in the number of small vacuoles.

As previously mentioned, during the dissociation proce-

dures, cells were produced that had lost their outer segment but appeared well preserved in all other respects. In the endings of these cells, very few synaptic vesicles were labeled with HRP. It is interesting to note that in contrast to intact photoreceptors, a small number of tracer-filled vesicles were also seen after illumination. Thus, cells deprived of their outer segment, not surprisingly, responded poorly to dark and were unable to react differentially to light exposure.

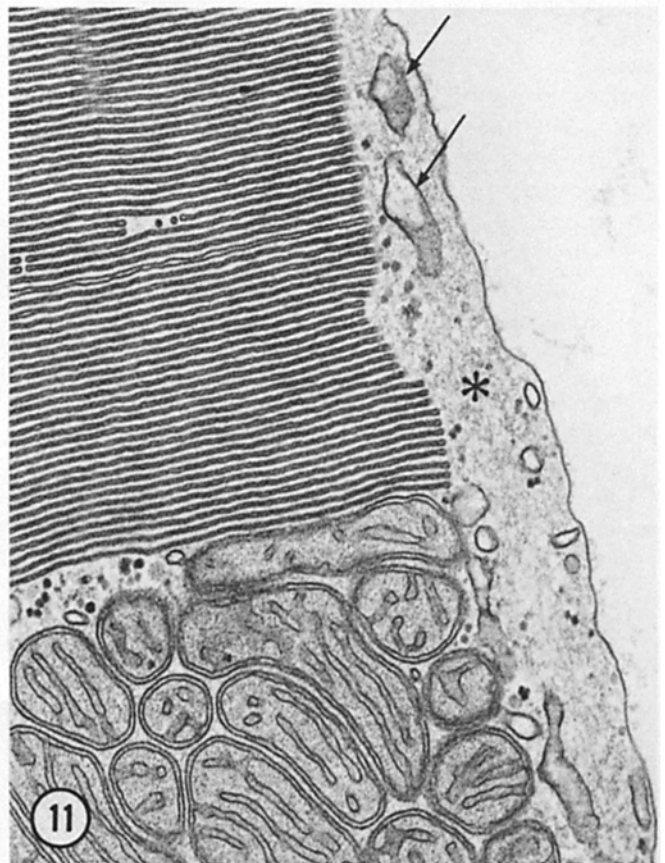
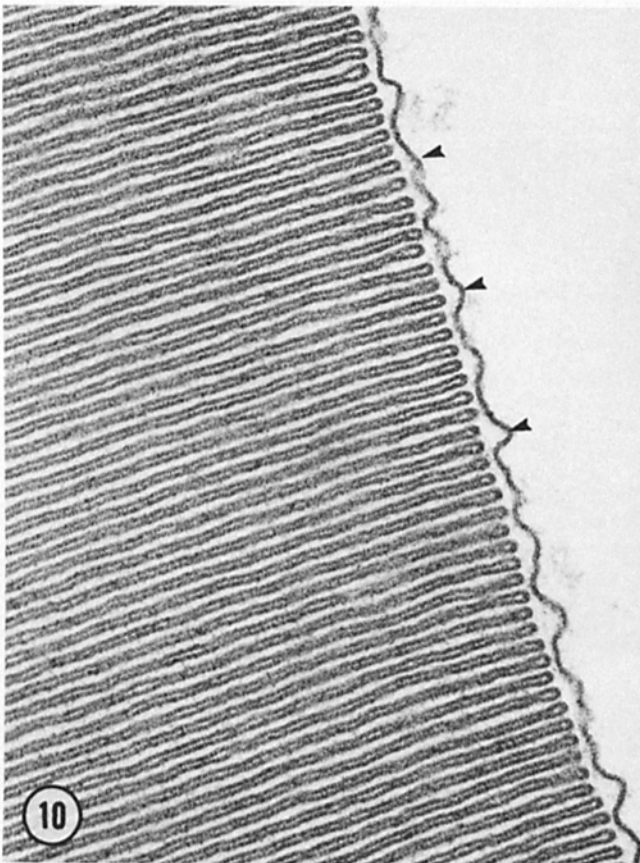
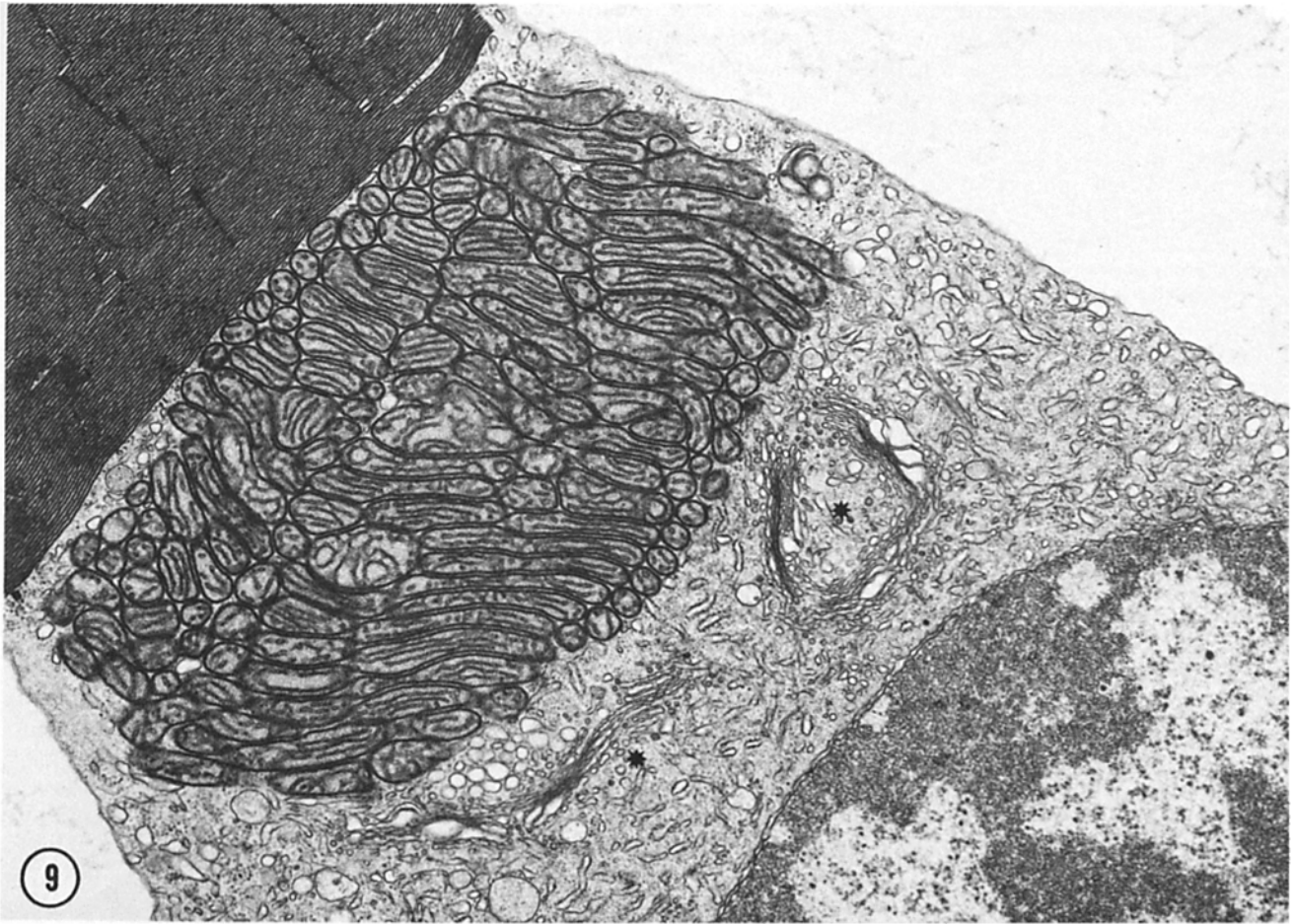
Dissociated Rod Cells in Long-term Cultures

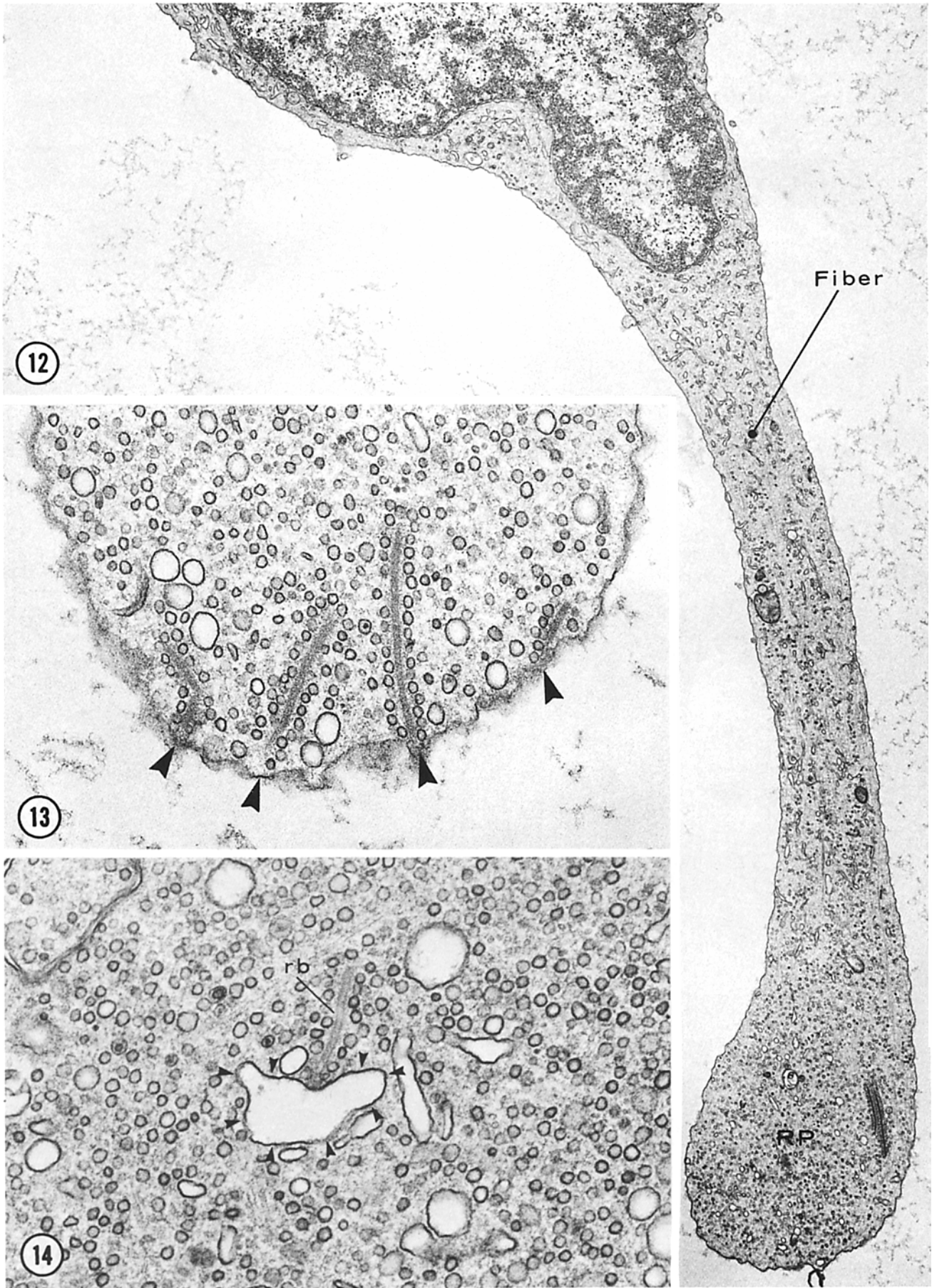
Cultures of solitary rod cells were examined at 24 h, 1 wk, and 2 wk. Throughout this period, the stack of membranous disks in the outer segment remained intact; however, a rearrangement of the cytoplasmic components and changes in the shape of the isolated rod photoreceptors were observed (Fig. 21). At 24 h, elements of the endoplasmic reticulum, small vesicles, ribosomes, and glycogen particles appeared in the peripheral cytoplasm of the outer segment around the edges of the membranous disks. These organelles presumably gained access to the outer segment through its broad connection with the inner segment. By 1 wk, the nucleus was eccentrically placed; indeed, in some cases, the cytoplasmic sleeve around the disks had enlarged to such an extent that the nucleus was found lying next to the stack of membranous disks (Fig. 21). By 2 wk, the ellipsoid also assumed an atypical location within the myoid, lying at some distance from the base of the outer segment; in addition, the cluster of mitochondria that make up the ellipsoid had begun to disperse. Pedicles were not seen in these cultures; however, a few synaptic ribbons were present in the perinuclear cytoplasm (Fig. 21, *inset*). Even at 2 wk, these ribbons were surrounded by a halo of vesicles and a few of them remained associated with the plasmalemma via a rudimentary arciform density. Thus, the overall impression gained from these cultures was that photoreceptors tended to round up with time but retained all their cytoplasmic constituents. The extensive shape changes seen here may be due to the poor adherence of the photoreceptors to most culture surfaces. In fact, recent observations suggest that normal cell

FIGURES 9–11 Rod cells 2 h after dissociation. Fig. 9: As in the intact retina, the inner segment contains an accumulation of mitochondria, a well-developed Golgi apparatus (*stars*), and numerous profiles of the endoplasmic reticulum. Note that the vacuoles have completely disappeared $\times 14,000$. Fig. 10: In the outer segment, the membranous disks are surrounded by the plasmalemma (*arrowheads*) and appear regularly stacked and flattened. $\times 97,500$. Fig. 11: Between the inner and outer segment, a cleft, continuous with the extracellular space, no longer exists and inner segment organelles are in direct contact with the membranous disks of the outer segment. A former calyceal process has become a narrow aisle of cytoplasm filled with microfilaments (*asterisk*). Membranous sacs, perhaps vestiges of the plasmalemma, are present within the filamentous mat. $\times 45,900$.

FIGURES 12–14 Rod cells 2 h after dissociation. Fig. 12: As in the intact retina, a rod pedicle (*RP*) is connected to the cell body by a fiber filled with microtubules and elements of the endoplasmic reticulum. $\times 6,500$. Fig. 13: The pedicle contains synaptic vesicles and vacuoles. Synaptic ribbons with their halo of synaptic vesicles remain attached to the surface of the ending (*arrowheads*). $\times 34,200$. Fig. 14: Ribbons (*rb*) are also found in the interior of the pedicle, associated with large membranous profiles (*arrowheads*). $\times 47,600$.

FIGURES 15–18 Computer reconstruction of pedicles from isolated rod cells. Fig. 15: This ending consists of a single pedicle; its connecting fiber is on the upper left. The central portion of the ending is rounded and gives rise to small digitations and large basal processes (*bp*). $\times 10,000$. Fig. 16: This ending consists of a double pedicle; the common connecting fiber is at the upper left. Both pedicles give rise to numerous small and large processes; only two basal processes are labeled (*bp*). $\times 6,200$. Fig. 17: In a portion of the ending in Fig. 15, the cytoplasmic contents are exposed. The membranous profiles associated with the synaptic ribbons represent cross sections of elongate sacs. Some of these sacs (*arrowheads*) open into the extracellular space (*arrow*) and thus represent deep invaginations of the cell surface. $\times 10,800$. Fig. 18: Slice through one pedicle of the ending in Fig. 16. Three synaptic ribbons (*rb*) are represented as arrays of dots. In this slice, two of them show their association with the cell surface; in one case this association occurs along a deep invagination of the plasmalemma (*arrowheads* and *arrow*). $\times 10,600$.





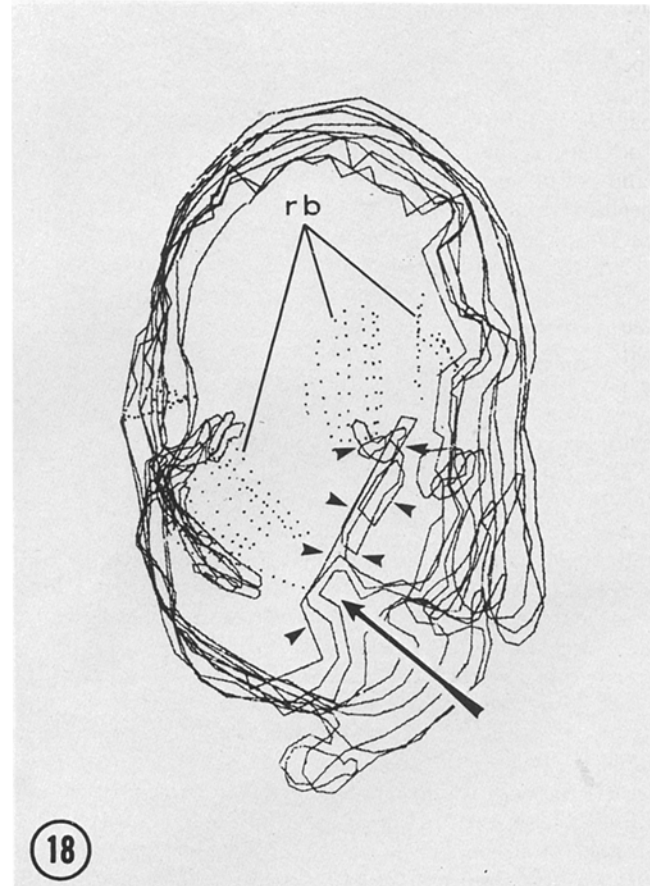
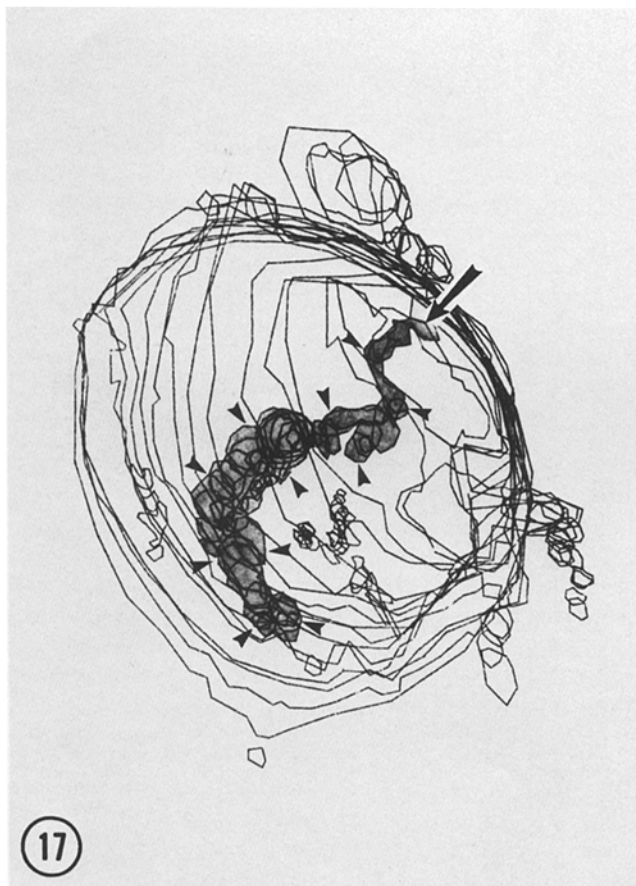
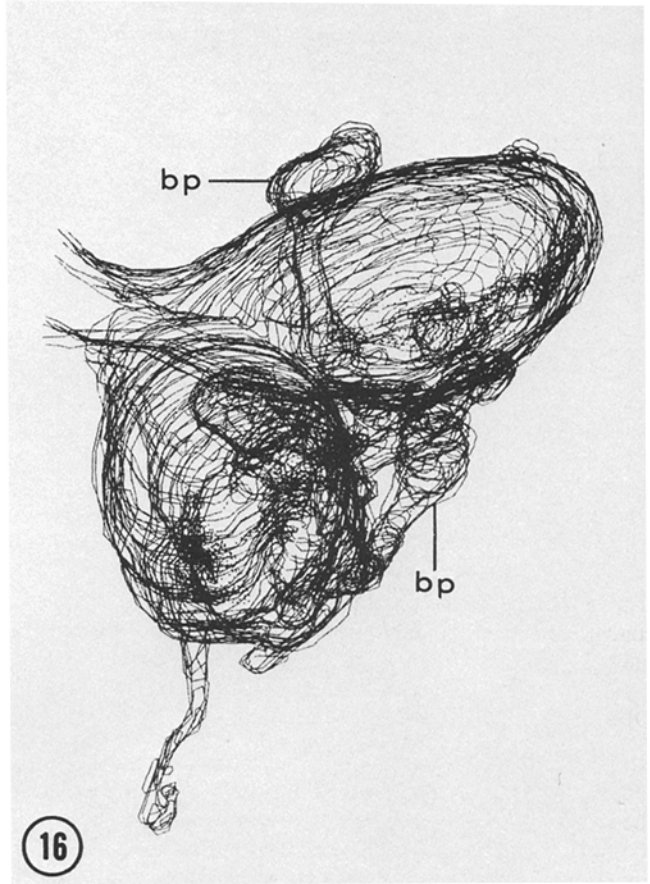
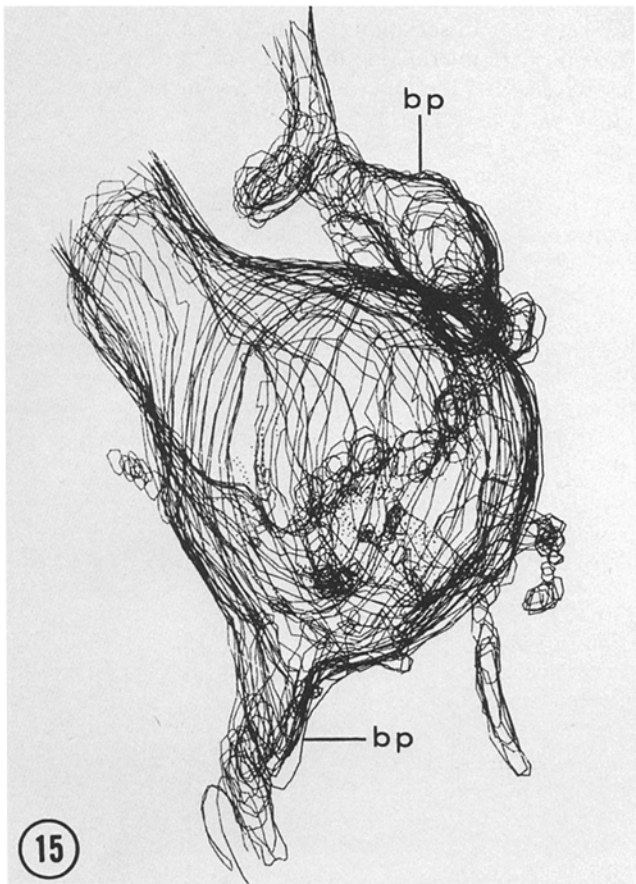


TABLE I
Localization of Synaptic Ribbons within the Synaptic Endings of Isolated Rod Cells*

	Single pedicle	Double pedicle [†]	Total
Total No. of ribbons (n)	7	9,6	22
No. of ribbons associated with the plasmalemma (n) [‡]	5	6,5	16
No. of ribbons associated with endocytic vacuoles (n)	2	3,1	6
Percentage of ribbons associated with the plasmalemma (%)	71.4	66.7, 83.3	72.7

* Data come from two rod cells that were dissociated from light-adapted retinas and maintained in the light at 10°C for 2 h. The synaptic endings were serially sectioned and reconstructed using three-dimensional computer graphics. One ending consisted of a single pedicle; the other contained two pedicles joined by a common fiber.

[†] The number of ribbons and percentages are given separately for each pedicle.

[‡] Association of the synaptic ribbon with the plasmalemma of the synaptic ending occurred either on the cell surface or along its invaginations.

shape is retained when photoreceptors are cultured on surfaces coated with a monoclonal antibody raised against retinal cell membranes (20).

DISCUSSION

Rod cells dissociated from the adult salamander retina were remarkably similar in fine structure to their counterparts in the intact retina. Two changes, however, were observed. First, the fins that radiate from the cell body just above the outer limiting membrane were lost during the dissociation procedure. As described in other species (17, 21), gap junctions connect the fins of adjacent photoreceptors. These surface specializations vigorously resist common dissociation techniques (22, 23); because of this strong mechanical adhesion, pairs of fins are most probably sheared or torn from the cell body during mechanical trituration. The transient accumulation of phagocytic vacuoles within the myoid of otherwise healthy-looking rod cells may indeed relate to the reorganization of the plasmalemma in this region.

The second change caused by dissociation took place at the junction between the inner and outer segments: the apex of the inner segment, including its calyceal processes, merged with the base of the outer segment. This event probably took place during the dissociation procedure, in that it was already present in rod cells fixed 1 h after isolation. The broad cytoplasmic continuity between inner and outer segments described here is not a unique feature of isolated photoreceptors: a cytoplasmic bridge joining inner and outer segments has been observed in the rods and cones of several mammalian retinas (24) and in at least one amphibian species (Richardson, T., Harvard Medical School, personal communication). Comparable cytoplasmic bridges, however, were not observed in the intact salamander retina.

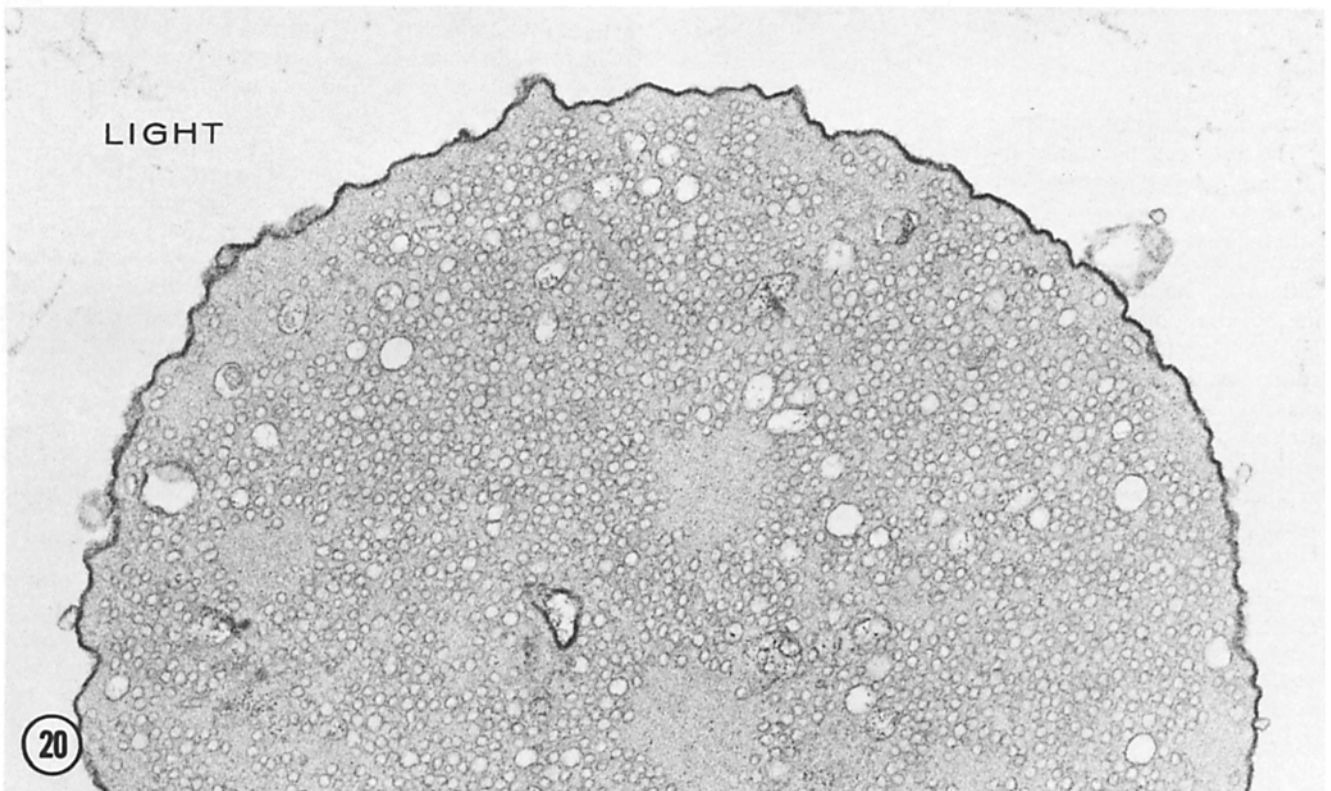
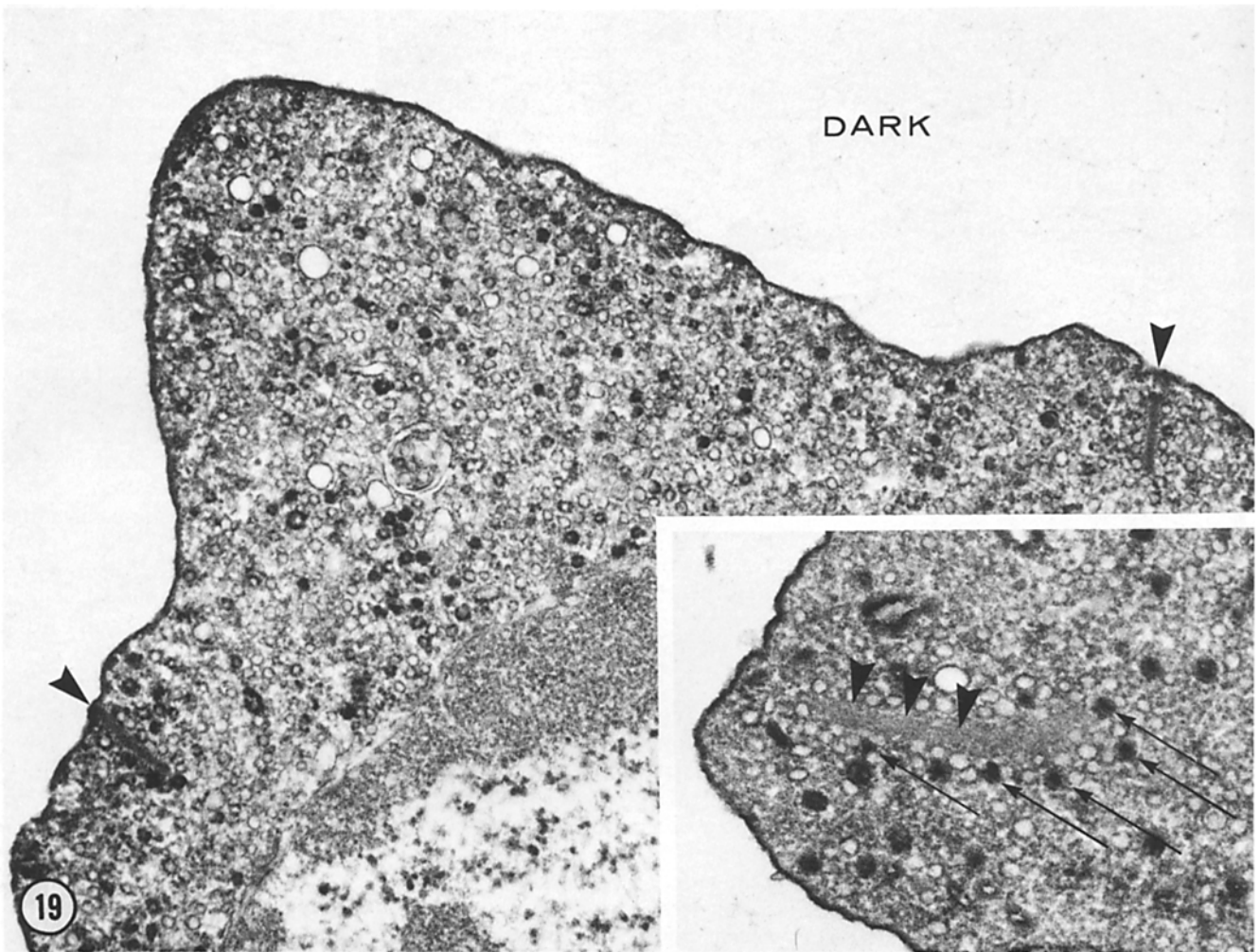
The broad fusion of inner and outer segments may affect some physiological properties of the photoreceptors. For instance, the ability of rod cells to renew their membranous disks could be inhibited. In fact, in our long-term cultures, we did not observe any lengthening of the outer segment but instead the slow envelopment of the base of the outer segment by the cytoplasm of the inner segment. Further, the axial electrical properties of the photoreceptors may be changed; this, however, does not seem to be the case, for salamander

rod cells are effectively isopotential both in the intact retina (25) and after dissociation (3). Finally, as a result of the broad fusion, some intermixing may take place of the membrane constituents of the inner and outer segments, which in the intact retina differ in lipid composition (26), ion permeation sites (cf. 27), and rhodopsin content (28).

In the pedicles of isolated rod cells about three-quarters of the synaptic ribbons remained associated with the plasmalemma at short time intervals after dissociation and some ribbons were found at the cell surface even after 2 wk in culture. Synaptic ribbons most probably function in concentrating synaptic vesicles at strategic sites of the surface of the endings; thus, their association with the pedicle membrane after removal of the postsynaptic neurons suggests that isolated receptors retain their presynaptic active zones. A parallel conclusion was reached in the neuromuscular junction for the postsynaptic specializations because receptors remain clustered after removal of the presynaptic axon terminal (29, 30). These experiments, however, were carried out on denervated muscle, in a procedure that leaves an intact basal lamina along the surface of the muscle cell (31); this structure may function as an organizing substrate that directs the regeneration of synaptic junctions (32, 33). In neuromuscular junctions dissociated with collagenase and protease, the basal lamina is no longer detectable at the electron microscope (34); nonetheless, there is no reduction in acetylcholine sensitivity, no change in the appearance of the postjunctional folds (34), and no decrease in the density of α -bungarotoxin binding along the crests of the folds (35). Thus, results from both the neuromuscular junction and solitary photoreceptors indicate that at least some components of the pre- and postsynaptic active zones are retained after enzymatic disjunction of mature synapses.

In the dark, solitary rod photoreceptors incorporated HRP, a tracer of the extracellular space, into synaptic vesicles and this uptake was suppressed by light; thus, they respond to changes in illumination as do the photoreceptors in the intact retina (36–38). Moreover, the maximal percentage of labeled vesicles in isolated photoreceptors is remarkably close to that observed in the intact retina: 40% in the dark and none in the light, as compared with 38% in the dark and 5% in light for skate (36) and frog (37) rod cells in situ. In the dark, the endings of isolated rod cells contained labeled coated vesicles and vacuoles, and, in the light, unlabeled vacuoles increased in number; all these phenomena, which are related to the process of recycling of synaptic vesicle membrane, also occur in the intact retina (36, 38). The tracer experiments strongly suggest, therefore, that isolated rod cells retain functional synaptic endings, releasing transmitter by synaptic vesicle exocytosis in the dark, and recycling constituents of the vesicular membrane after the fusion event with the plasmalemma. It remains to be proven, however, that the transmitter substances are indeed contained in the interior of the synaptic vesicles.

In solitary rod cells, maximal uptake of HRP took place in cells that had been previously light-adapted, were maintained at low temperature, and exposed to low concentrations of Ca^{++} . The effect of increasing the temperature to 18 and 22°C was dramatic: endocytosis of tracer was completely inhibited. This sharply contrasts with the results from the intact retina of cold-blooded vertebrates where good uptake was achieved at 20–25°C (37, 38). Although the fine structure of single rod cells maintained at 18 and 22°C appeared nor-



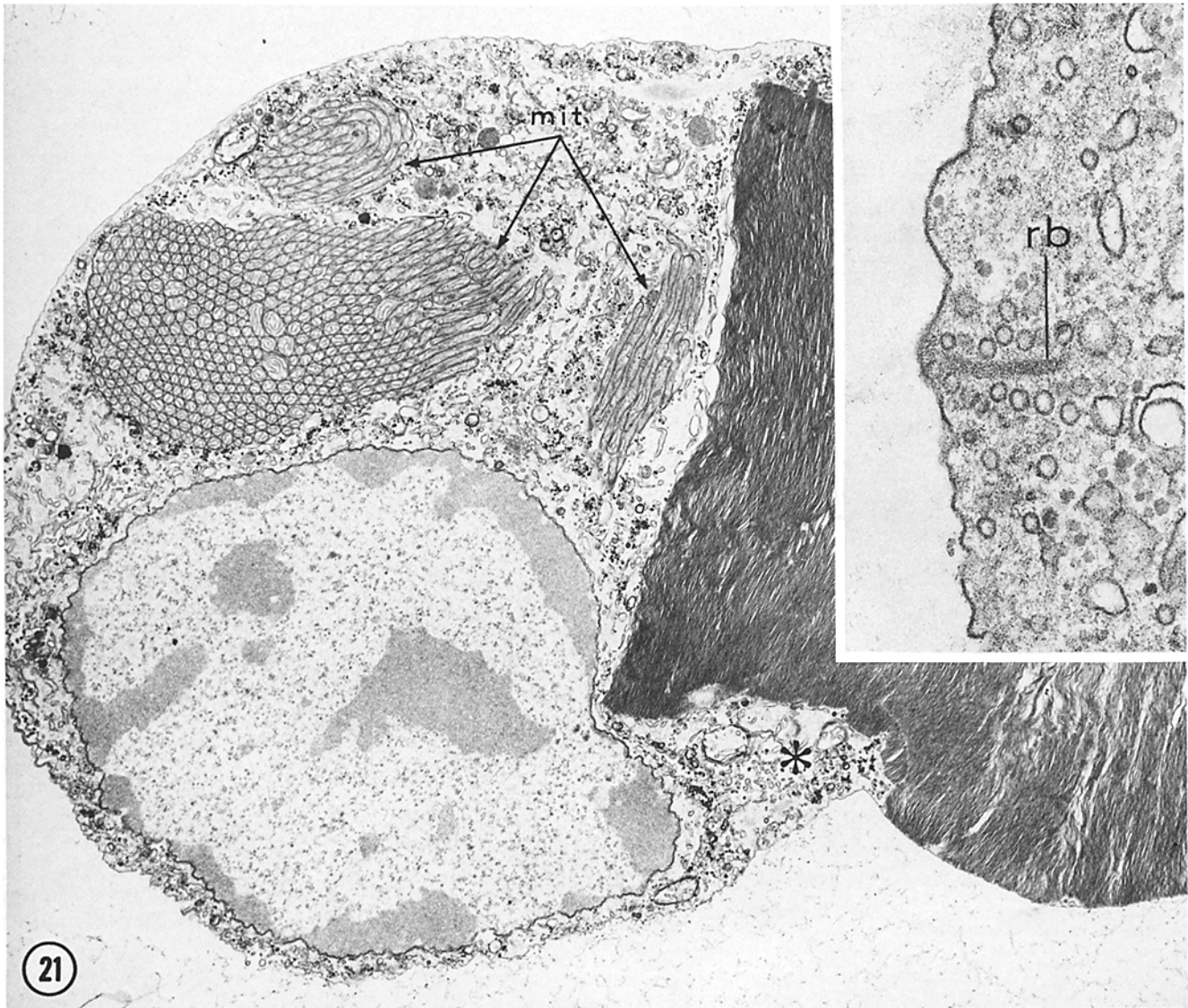


FIGURE 21 Long-term culture of solitary rod cells. After 2 wk in culture, the nucleus is eccentrically placed, the accumulation of mitochondria (*mit*) that forms the ellipsoid is fragmented, and cell organelles are present along the edges of the membranous disks (*asterisk*). Nonetheless, the cell is recognizable as a rod photoreceptor and retains its stack of disks in the outer segment; (*inset*) a synaptic ribbon (*rb*) remains attached to the cell surface 1 wk after dissociation from the retina. $\times 5,800$; (*inset*) $\times 67,000$.

mal, solitary receptors do deteriorate at these temperatures with time. The lack of tracer uptake could be an early sign of this deterioration. The effects of previous dark adaptation or high Ca^{++} concentration were less severe: rod cells in these conditions did contain a small number of labeled synaptic vesicles. The increase in HRP uptake with low Ca^{++} may be a result of the known effects of this ion on the membrane potential of rod cells (39, 40): the photoreceptors are more depolarized in low Ca^{++} and this in turn would stimulate synaptic vesicle exocytosis. The reason for the increase of HRP uptake in cells that were light-adapted at the time of incubation in the tracer is unclear. Perhaps solitary rod cells

maintained in the dark and thus synaptically active, gradually deplete their store of a necessary metabolite. Alternatively, the cells may possess an intrinsic mechanism that controls transmitter release in the dark. In this context it is interesting to note that in the intact chick retina, the surface of the rod synaptic endings first increases and then decreases upon dark exposure (41). This can be explained by changes in the rate of synaptic vesicle exocytosis and recycling as the photoreceptor becomes dark-adapted. The possibility that tracer uptake by synaptic vesicles may increase upon intermittent light stimulation should be explored.

Isolated rod cells that lack an outer segment do not respond

FIGURES 19 and 20 Tracer uptake by isolated rod cells. Fig. 19: After incubation with HRP in the dark, numerous synaptic vesicles are filled with the tracer. The labeled vesicles are found scattered throughout the matrix of the pedicle as well as attached to synaptic ribbons (*inset*, *arrows*). Note that in this instance, the rod pedicle is fused with the cell body. Arrowheads indicate synaptic ribbons. $\times 29,000$; (*inset*) $\times 48,000$. Fig. 20: Illumination suppresses the uptake of HRP. Tracer, however, adheres to the outer aspect of the plasma membrane. $\times 28,400$.

differentially to light and dark, and in both conditions contain only a few labeled synaptic vesicles. Thus, they have lost the ability to vary their membrane potential in response to changes in illumination. This finding, further supports the idea that tracer uptake by intact solitary photoreceptors is a good indicator of functional integrity after dissociation.

The authors thank Ms. Suzanne Kuffler for her excellent technical assistance with the computer graphics reconstructions and Mr. Peter Ley for photographic assistance. This work was supported by grants EY 05521, EY 03665, and EY 01344 from the National Institutes of Health.

Received for publication 27 February 1984, and in revised form 5 July 1984.

REFERENCES

- Bader, C. R., P. R. MacLeish, and E. A. Schwartz. 1978. Responses to light of solitary rod photoreceptors isolated from tiger salamander retina. *Proc. Natl. Acad. Sci. USA* 75:3507-3511.
- MacLeish, P., M. Tachibana, and E. Townes-Anderson. 1982. Morphological and electrophysiological properties of dissociated retinal neurons. *In Adv. Pharmacol. Ther.* 2:245-253.
- Bader, C. R., P. R. MacLeish, and E. A. Schwartz. 1979. A voltage-clamp study of the light response in solitary rods of the tiger salamander. *J. Physiol. (Lond.)*, 296:1-26.
- Werblin, F. S. 1979. Time- and voltage-dependent ionic components of the rod response. *J. Physiol. (Lond.)*, 294:613-626.
- Attwell, D., and M. Wilson. 1980. Behaviour of the rod network in the tiger salamander retina mediated by membrane properties of individual rods. *J. Physiol. (Lond.)*, 309:287-315.
- Townes-Anderson, E., P. R. MacLeish, and E. Raviola. 1982. Solitary rod photoreceptors of the tiger salamander: ultrastructure and uptake of horseradish peroxidase (HRP). *J. Cell Biol.* 95:140a. (Abstr.)
- Townes-Anderson, E., P. R. MacLeish, and E. Raviola. 1983. Structure and function of solitary rod photoreceptors. *Invest. Ophthalmol. Vis. Sci.* 24(Suppl.):257.
- Stebbins, R. C. 1951. Amphibians of Western North America. University of California Press, Berkeley. 29-49.
- Karnovsky, M. J. 1971. Use of ferrocyanide-reduced osmium tetroxide in electron microscopy. Abstracts of the Eleventh Annual Meeting, The American Society for Cell Biology. 146.
- Lam, D. M. K. 1972. Biosynthesis of acetylcholine in turtle photoreceptors. *Proc. Natl. Acad. Sci. USA*, 69:1987-1991.
- Bray, D. 1970. Surface movements during the growth of single explanted neurons. *Proc. Natl. Acad. Sci. USA*, 65:905-910.
- Ito, S., and M. J. Karnovsky. 1968. Formaldehyde-glutaraldehyde fixatives containing trinitro compounds. *J. Cell Biol.* 39:168a. (Abstr.)
- Gilbert, C. D., and T. N. Wiesel. 1983. Clustered intrinsic connections in cat visual cortex. *J. Neurosci.* 3:1116-1133.
- Graham, R. C., Jr., and M. J. Karnovsky. 1966. The early stages of absorption of injected horseradish peroxidase in the proximal tubules of mouse kidney: ultrastructural cytochemistry by a new technique. *J. Histochem. Cytochem.* 14:291-302.
- Adams, J. C. 1977. Technical considerations on the use of horseradish peroxidase as a neuronal marker. *Neuroscience*, 2:141-145.
- Laurens, H., and J. W. Williams. 1917. Photomechanical changes in the retina of normal and transplanted eyes of *Amblystoma* larvae. *J. Exp. Zool.* 23:71-83.
- Custer, N. V. 1973. Structurally specialized contacts between the photoreceptors of the retina of the axolotl. *J. Comp. Neurol.* 151:35-56.
- Lasansky, A. 1973. Organization of the outer synaptic layer in the retina of the larval tiger salamander. *Philos. Trans. R. Soc. London Ser. B. Biol. Sci.* 265:471-489.
- Szamer, R. B., and H. Ripps. 1983. The visual cells of the skate retina: Structure, histochemistry, and disc-shedding properties. *J. Comp. Neurol.* 251:57-62.
- MacLeish, P. R., C. J. Barnstable, and E. Townes-Anderson. 1983. Use of a monoclonal antibody as a substrate for mature neurons *in vitro*. *Proc. Natl. Acad. Sci. USA*, 80:7014-7018.
- Gold, G. H., and J. E. Dowling. 1979. Photoreceptor coupling in retina of the toad, *Bufo marinus*. I. Anatomy. *J. Neurophysiol.* 42:292-310.
- Pfenninger, K. H. 1971. The cytochemistry of synaptic densities. II. Proteinaceous components and mechanism of synaptic connectivity. *J. Ultrastruct. Res.* 35:451-475.
- Fischbach, G. D., and P. G. Nelson. 1977. Cell culture in neurobiology. *Handb. Physiol. (Sect. 1, Nerv. Syst.)* 1(Pt. 2):719-774.
- Richardson, T. M. 1969. Cytoplasmic and ciliary connections between the inner and outer segments of mammalian visual receptors. *Vision Res.* 9:727-731.
- Werblin, F. S. 1978. Transmission along and between rods in the tiger salamander retina. *J. Physiol. (Lond.)*, 280:449-470.
- Andrews, L. D., and A. I. Cohen. 1983. Freeze-fracture studies of photoreceptor membranes: New observations bearing upon the distribution of cholesterol. *J. Cell Biol.* 97:749-755.
- Bader, C. R., D. Bertrand, and E. A. Schwartz. 1982. Voltage-activated and calcium-activated currents studied in solitary rod inner segments from the salamander retina. *J. Physiol. (Lond.)*, 331:253-284.
- Peters, K.-R., G. E. Palade, B. G. Schneider, and D. S. Papermaster. 1983. Fine structure of a periciliary ridge complex of frog retinal rod cells revealed by ultrahigh resolution scanning electron microscopy. *J. Cell Biol.* 96:265-276.
- Frank, E., K. Gautrik, and H. Sommerschild. 1975. Cholinergic receptors at denervated mammalian motor end-plates. *Acta Physiol. Scand.* 95:66-76.
- Porter, C. W., and E. A. Barnard. 1975. Distribution and density of cholinergic receptors at the motor endplates of a denervated mouse muscle. *Exp. Neurol.* 48:542-556.
- Nickel, E., and P. G. Waser. 1968. Elektronen mikroskopische Untersuchungen am Diaphragma der Maus nach einseitiger Phrenikotomie. I. Die degenerierende motorische Endplatte. *Z. Zellforsch. mikrosk. Anat.* 88:278-296.
- Sanes, J. R., L. M. Marshall, and U. J. McMahan. 1978. Reinnervation of muscle fiber basal lamina after removal of myofibers. Differentiation of regenerating axons at original synaptic sites. *J. Cell Biol.* 78:176-198.
- Burden, S. J., P. B. Sargent, and U. J. McMahan. 1979. Acetylcholine receptors in regenerating muscle accumulate at original synaptic sites in the absence of the nerve. *J. Cell Biol.* 82:412-425.
- Betz, W., and B. Sakmann. 1973. Effects of proteolytic enzymes on function and structure of frog neuromuscular junctions. *J. Physiol. (Lond.)*, 230:673-688.
- Lentz, T. L., J. E. Mazurkiewicz, and J. Rosenthal. 1977. Cytochemical localization of acetylcholine receptors at the neuromuscular junction by means of horseradish peroxidase-labeled α -bungarotoxin. *Brain Res.* 132:423-442.
- Ripps, H., M. Shakib, and E. D. MacDonald. 1976. Peroxidase uptake by photoreceptor terminals of the skate retina. *J. Cell Biol.* 70:86-96.
- Schächer, S., E. Holtzman, and D. C. Hood. 1976. Synaptic activity of frog retinal photoreceptors. A peroxidase uptake study. *J. Cell Biol.* 70:178-192.
- Schaeffer, S. F., and E. Raviola. 1978. Membrane recycling in the cone cell endings of the turtle retina. *J. Cell Biol.* 79:802-825.
- Yoshikami, S., and W. A. Hagins. 1973. Control of the dark current in vertebrate rods and cones. *In Biochemistry and Physiology of Visual Pigments*. H. Langer, editor. Springer Verlag, Berlin. 245-255.
- Brown, J. E., and L. H. Pinto. 1974. Ionic mechanism for the photoreceptor potential of the retina of *Bufo marinus*. *J. Physiol. (Lond.)*, 236:575-591.
- Cooper, N. G. F., and B. J. McLaughlin. 1982. Structural correlates of physiological activity in chick photoreceptor synaptic terminals: effects of light and dark stimulation. *J. Ultrastruct. Res.* 79:58-73.